

Numerical simulation of shot peening process: influence of the constitutive model of the target material

PEÑUELAS, I.*, RODRÍGUEZ, C., GARCÍA, T.E., BELZUNCE, F.J.

Mechanical and Civil Engineering

University of Oviedo

Polytechnic School of Engineering - Campus de Gijón, 33203

SPAIN

penuelasines@uniovi.es, www.simumecamat.com/

Abstract: - This paper analyse the effect of the constitutive material model used to describe the target material on the results obtained from numerical simulation of shot peening process. From experimental characterization of a duplex stainless steel, including both high rate monotonic tests and low cyclic fatigue tests, three constitutive models are proposed and incorporated into a FE simulation. Numerical predictions of residual stresses and roughness, and experimental results are compared. Best results were obtained using a non-linear kinematic–isotropic model which combines the effect of the cyclic deformation produced by repeated impacts with the strain rate effect through its isotropic component. The only consideration of the effect of the strain rate, overestimate the experimental values of residual stress. On the other hand, if only the cyclic loading effect is taken into account, numerical predictions underestimate the actual residual stresses values.

Key-Words: - Shot peening, Duplex stainless steel, Constitutive model, Numerical simulation

1 Introduction

Shot peening process (SP) is one of the most widely used mechanical surface treatments applied to improve the fatigue behaviour of metallic components. This process generates a cold plastic deformation on the surface of the working piece, by peening it with small spherical shots that impact on this surface at high speed. The large localized plastic deformation on the surface of the material produces a compressive residual stresses field [1, 2], affecting the fatigue behaviour of the material. The shot peening process depends on so many factors and their influence is so complex to analyse, that usually is not feasible from the economic point of view to study each effect just by means of experimental testing. Thus the numerical analysis by means of the finite element method is an interesting complementary alternative to develop a complete study of the process. However, the numerical simulation is really complex, since shot peening is a dynamic problem in which multiple impacts are involved and a high computational cost is required.

One of the main factors when modelling this process is the constitutive model used to describe the behaviour of the target material. On the one hand, the material is subjected to shots that impact the surface at high speeds, so it is necessary to use constitutive material models sensitive to the effect of the strain rate. These models are described by

isotropic hardening laws. However, isotropic models are only valid if the load process during the test is monotonic, or in case of cyclic loads where Bauschinger effects are not present. Since the shot peening process is based on the action of repeated loads, the cyclic response of the material should be taken into account. If the material does not exhibit the Bauschinger effect, the use of an isotropic model may be right; otherwise, a kinematic hardening model should be used. Despite the relevance of using the best constitutive material model for each case, researchers working on the modelling of shot peening process still have not achieved the best way to address the problem. Most studies use isotropic hardening models, which do not take into account the cyclic behaviour of the target material [3–7] and others, use only kinematic models, which do not consider strain rate effects [8–11].

The aim of the present study is to analyse the effect of the constitutive material model used to describe the mechanical behaviour of the target material, on the results obtained from the numerical modelling of the shot peening process. This will involve the whole experimental characterization of duplex stainless steels, as well as the proposal of different constitutive models based on the type of applied load: monotonic dynamic load or cyclic loading. Once considered in finite element analyses, the goodness of each constitutive model will be

analysed by comparing the numerical predictions for residual stresses and surface roughness with corresponding experimental results.

2. Material and constitutive models

2.1 Material and experimental characterization

The material used in this study is a duplex (AISI 2205 grade) stainless steel, supplied as hot rolled bars, with nominal diameter 16 mm. The chemical composition of this steel is shown in Table 1.

Table 1. Chemical composition of the steel (% max)

C	Si	Mn	Cr	Ni	Mo	Ti	Cu	N	Co	Nb	V	S	P
0.019	0.34	1.67	22.23	4.84	3.33	0.025	0.26	0.17	0.087	0.014	0.11	0.001	0.026

Metallographic analyses performed on longitudinal and transversal sections of the bars show a duplex α/γ microstructure (50%/50%). Static tension tests were carried out accordingly to ASTM E8M [10] in order to obtain the monotonic properties of the material (Young's Modulus, E ; yield stress, σ_y ; ultimate tensile stress, σ_u ; tensile elongation e ; reduction of area, z). The results are given in Table 2, as well as Vickers hardness of the material ($HV_{0.5}$).

Table 2. Tensile properties and Vickers hardness of the steel

Material	E (MPa)	σ_y (MPa)	σ_u (MPa)	ϵ (%)	Z (%)	$HV_{0.5}$
D2205	192433	632	799	37.92	75.79	275

In addition, the influence of the strain rate on the mechanical behaviour of the material was assessed using monotonic tension and/or compression tests performed at four different strain rates: 0.00085 s^{-1} , 0.02 s^{-1} , 0.09 s^{-1} and 850 s^{-1} . Standard cylindrical samples [12] were used to carry tensile tests in order to evaluate the effect of the three lower strain rates. In the case of the highest strain rate, were carried out Hopkinson's bar compression tests. The effect of each strain rate was analysed using a minimum of three samples. Fig.1. show the obtained stress-strain curves.

The plastic response of the material was assessed by means of series of cyclic tension-compression tests under strain control, using a sine waveform [13]. Low-cycle symmetric fatigue tests ($R = -1$) were performed up to the stabilized cycle at different deformation intervals ($\Delta\epsilon = \pm 0.0035$, ± 0.004 , ± 0.0045 , ± 0.05 , ± 0.055 and $\pm 0.06 \text{ mm/mm}$). In order to determine whether the cyclic plastic response of the material is affected or not by the strain rate, tests were performed at two different

strain rates: 0.00085 s^{-1} and 0.02 s^{-1} . The small effect of strain rate shown in monotonic stress-strain curves for the two lower strain rates 0.00085 s^{-1} and 0.02 s^{-1} is not observe for cyclic response, where the differences are negligible.

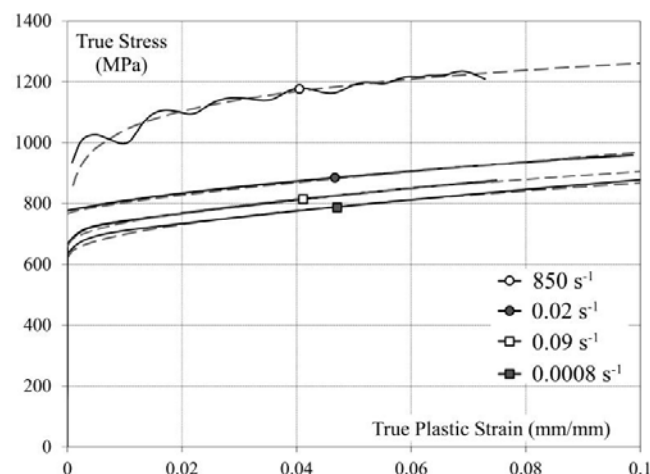


Fig.1. Typical stress-plastic strain curves obtained in tension or compression tests at different strain rates and Johnson-Cook model predictions (dashed lines).

Fig. 2 shows the cyclic hardening curve (dashed line) plotted from the stabilised cyclic tension-compression curves obtained from tests performed at 0.00085 s^{-1} . Fig.2 also shows the monotonic hardening curve (solid line) obtained from the monotonic tension tests at same strain rate.

2.2 Constitutive models

2.2.1. Isotropic constitutive model: only strain rate effect

The effect of strain rate on the mechanical response of the material was modelled using the isotropic constitutive models: Cowper-Symonds [14], Johnson-Cook [15] and their modified versions [16, 17]. Johnson-Cook model is the one that that best represented the behaviour of our material at any strain rate. This model writes the evolution of the hardening plastic surface, σ , in terms of the equivalent plastic strain, $\bar{\epsilon}^p$, and the dimensionless equivalent plastic strain rate, $\dot{\bar{\epsilon}}^p$:

$$\sigma = [A + B(\bar{\epsilon}^p)^n] \cdot [1 + C \ln(\dot{\bar{\epsilon}}^p / \dot{\bar{\epsilon}}_o^p)] \quad (1)$$

Where $\dot{\bar{\epsilon}}_o^p$ is the reference plastic strain rate, and A , B , C , n are model parameters. Table 3 shows the values of model parameters that best fit the experimental results. The Johnson-Cook model

predictions obtained using these parameters at different strain rates are shown in Fig. 1.

Table 3. Experimental parameters of the Johnson-Cook model

A (MPa)	B (MPa)	C	n
622	785.25	0.035	0.5046

2.2.2. Isotropic-kinematic constitutive model: only cyclic plastic response

The experimental results (Fig. 2) show the strong Bauschinger effect (after prior yielding in tension, yielding in compression starts at a lower stress level than the initial compression yield stress) exhibited by the analysed material. Thus, it is necessary to use a kinematic hardening model to describe this material.

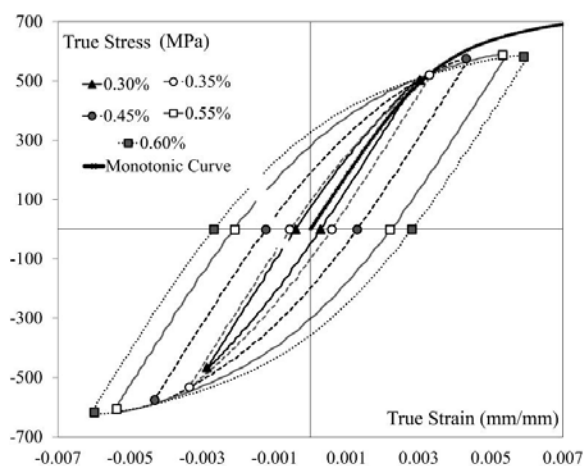


Fig.2. Monotonic and cyclic behaviour of the material at strain rate 0.00085 s⁻¹

The model assumes that the yield surface is displaced from its original position in the principal stress space. In addition, the size of the plastic surface also changes and the material undergoes cyclic softening (Fig.2). This plastic behaviour of the material under cyclic loading was modelled using a non-linear combined isotropic-kinematic hardening formulation, first introduced by Armstrong and Fredrick and subsequently modified by Chaboche [18]. This model expresses the evolution of the back-stress tensor, X, as a function of the equivalent plastic strain rate:

$$\dot{X} = C \frac{1}{\sigma_0} (\sigma - X) \dot{\epsilon}^p - \gamma X \dot{\epsilon}^p \quad (2)$$

Where C and γ are model parameters and σ_0 the size of the yield surface.

In the case analysed here, where the material shows cyclic softening, the evolution of the yield surface size is described by the expression:

$$\sigma^0 = \sigma|_0 + Q_\infty (1 - e^{-b\bar{\epsilon}^p}) \quad (3)$$

Where $\sigma|_0$ is the yield stress (for a plastic strain equal to zero) in the first cycle, and Q_∞ and b are experimental parameters. The detailed procedure to obtain all the model parameters can be seen in the references [19].

Table 4. Parameters of the isotropic-kinematic Chaboche model

$\dot{\epsilon}$ (s ⁻¹)	C (MPa)	γ	Q_∞ (MPa)	b
0.00085	193556	584	-24	12
0.02	192772.4	575.44	-23	13

Table 4 shows the model parameters obtained from the two strain rates used in the cyclic tests and from the tests performed at $\Delta\epsilon = \pm 0.0045$. Since there are no significant differences between the parameter values corresponding to both strain rates, the values obtained for the higher strain rate (0.02 s⁻¹) were adopted.

2.2.3. Proposed constitutive model: strain rate and cyclic loading effects

Shot-peened materials are subjected to the combined effects of the strain rate and cyclic loads, so their constitutive model should include both effects. Therefore, the model proposed in this paper uses the isotropic component of the isotropic-kinematic Chaboche model, σ_0 , to include the strain rate effect. From Eq. (3) and given that the parameters Q_∞ and b do not seem to be affected by the strain rate (Table 4), the effect of this variable will be incorporated via the value of $\sigma|_0$ (yield stress value for a plastic strain equal to zero) obtained at the different strain rates. Table 5 shows the experimental values of $\sigma|_0$ obtained from the monotonic tests.

3 Shot peening process

3.1. Experimental characterization

Duplex stainless steel discs (16 mm diameter and 10 mm thickness) extracted from bars were subjected to a shot peening process using a GUYSON Euroblast 4PF direct pressure pneumatic machine and S-230 steel shots with a nominal diameter of 0.6 mm. The air pressure, shot flow and distance

between the nozzle and specimen were chosen to achieve a13A Almen Intensity SAE J442 [20] and SAE J443 [21].

Tabla 5. σ_{l_0} Values at different strain rates

	$\dot{\epsilon} = 0.0008s^{-1}$	$\dot{\epsilon} = 0.02s^{-1}$	$\dot{\epsilon} = 0.09s^{-1}$	$\dot{\epsilon} = 850s^{-1}$
σ_{l_0} (MPa)	440	488	630	800

The numerical model requires data of the diameters of the shots and the velocity at which they exit the nozzle were carried out. Thus, accurate measurements of both test parameters were carried out. The diameter and shape of the shots were measured using image analysis techniques. In all, 701 shots were characterised. Statistical analysis by means of the SPSS software showed a normal distribution of shot diameters with a mean value of 0.79 ± 0.051 mm. Shot shape was determined using MIL-S-13165-C [22] and SAE J2441 [23] specifications and showed a shape factor value of 0.86 ± 0.031 . In order to obtain the velocity of the Shots exiting the nozzle, an experimental device based on the use of photoelectric sensors [24] was used. This device was placed at the nozzle outlet and it measured the time that a shot requires to travel a specified distance between two light beams. The analysis of 250 characteristic peaks showed an average shot velocity of 44 ± 10 m/s at the nozzle outlet. Notwithstanding, as the distance between the nozzle outlet and the surface of the specimen to be peened is relatively small, the impact velocity may be considered equal to the speed at the outlet of the nozzle.

Table 6. Experimentally obtained in-depth residual stress values

Depth (mm)	Residual Stress (MPa)
0	-522.97 \pm 37.5
0.380	-659.77 \pm 51.4
0.800	-722.30 \pm 45.4
0.120	-705.17 \pm 45.1
0.160	-621.67 \pm 43.5
0.228	-549.23 \pm 53.7
0.288	-312.83 \pm 28.3
0.348	-151.60 \pm 22.2
0.400	63.37 \pm 24.8

In addition, two different coverage grades were used in this paper: very low coverage (<10%), necessary for determining the diameter of an isolated shot mark and Full coverage (98%), necessary for the standard description of the process. The time required for ensuring both coverage values were determined using the Avrami equation. Besides, the diameter of the dimple created by a single impact was obtained by image

analysis techniques using a minimum of 4 samples and measuring 40 isolated marks in all. The average diameter obtained was 260 ± 10 μ m.

The full coverage shot peening process provided the values of residual stresses and roughness. Residual stresses were obtained by X-ray diffraction analysis (XRD) of the surface layer of the as-treated samples using a Stresstech G3 X-Ray diffractometer (radiation Cr K α , irradiated area 1 mm², sin² ψ method, 11 diffraction angles (2θ) scanned between -45° and 45°). Measurements were performed in (2 1 1) planes for the ferrite phase and in (2 2 0) for austenite. Elastic moduli of 211 GPa (ferrite) and 196 GPa (austenite) were used [25]. The overall value of residual stress was obtained taking into account the volume fraction of the two phases and applying the rule of mixtures [26]. Table 6 summarizes the experimental results obtained. The maximum compressive stress value, 722.30 MPa, is obtained for a depth of 0.120 mm, while the surface residual stress is significantly lower at 522.97 MPa. The depth of the entire zone affected by the shot peening treatment is about 0.350 mm. All of these values are in line with the residual stress profile resulting from typical shot peening treatments.

The shot peening process also affects the roughness of the peened surface. Thus, it is interesting to determine the roughness parameters with a higher degree of sensitivity to topographical profile of the peened surface. It is recommended to use of the Rt parameter, i.e. the maximum height of the profile, which describes the distance between the highest peak and the deepest valley [27, 28]. The roughness values of the peened strips were obtained using both a Diavite DH-6roughness tester and a Leica DCM3D confocal microscope. A Class 1 precision (5%) roughness tester was used to obtain 4 roughness profiles with a length-measurement of 4.8 mm. The average value of Rt thus obtained was 16.66 μ m. Furthermore, three surface measurements were carried out using the confocal microscope, within an average area of 0.354 mm². In this case, the average value of Rt thus obtained was 15.36 μ m, showing great concordance with the result obtained using the roughness tester.

3.2. Numerical simulation

Numerical simulation was carried out using ABAQUS FEA commercial code. Since shot peening is a high speed process and dynamic effects should be taken into account, an explicit solver was used for simulations. Both, axisymmetric and 3D models were developed. The effect of the impact of a single shot was studied by means of the axisymmetric model. This model only focused on

the analysis of the material response under monotonic loads. The comparison of experimental and numerical results of the diameters of the dimples, allow checking the experimental measurement of shot velocity and provides an initial approximation of the validity of the different constitutive models. The target specimen was modelled as a cylinder with a radius of 2.25 mm and 1 mm in width (Fig.3). Axisymmetric 4-node elements with reduced integration (CAX4R) were used. In order to eliminate the size effect of the specimen, the reflections of the elastic waves produced by the shot were avoided using 4-node axisymmetric infinite elements (CINAX4), which were used to cover the bottom and lateral edges of the model [4, 11]. All degrees of freedom were restricted on the bottom edge. As the shot impact was simulated on the centre top of the specimen, the mesh was refined in this region using a minimum element size of 5 μm .

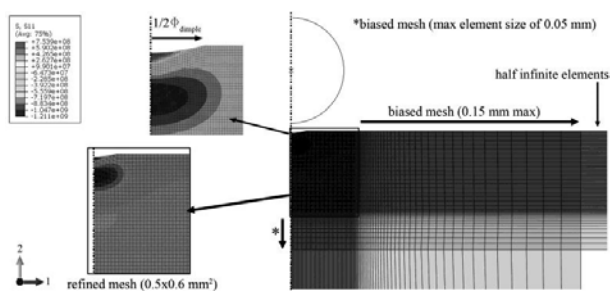


Fig.3. Scheme of the axisymmetric model after the impact of one shot

It is worth noting that in an actual shot peening process, the target material is subjected to a high number of random overlapped impacts all over its surface, so a 3D model is needed to simulate the impact of several shots. This model was used to obtain the residual stress profile (created under the surface) and the roughness of the peened material. The 3D target specimen was modelled as a rectangular body with a volume of $3 \times 3 \times 1.3 \text{ mm}^3$ (Fig.4) using 8-node continuum elements with reduced integration and hourglass control (C3D8R). Infinite elements (CIN3D8) were employed to cover the lateral and bottom faces. In addition, the degrees of freedom of the bottom face were restricted. The impact zone was reduced to a $1 \times 1 \times 0.6 \text{ mm}^3$ volume in the central zone of the specimen [11, 28]. A finer mesh was used in this region, with a minimum element volume of $12 \times 12 \times 15 \text{ }\mu\text{m}^3$. Other studies have revealed that a ratio between element size and dimple diameter of 1:20 offers good results for these impact simulations [11]. The 1 mm^2 impact surface was chosen taking into account the measured surface of the X-Ray diffractometer [11, 28] to

obtain a numerical profile of the residual stresses similar to the experimental profile.

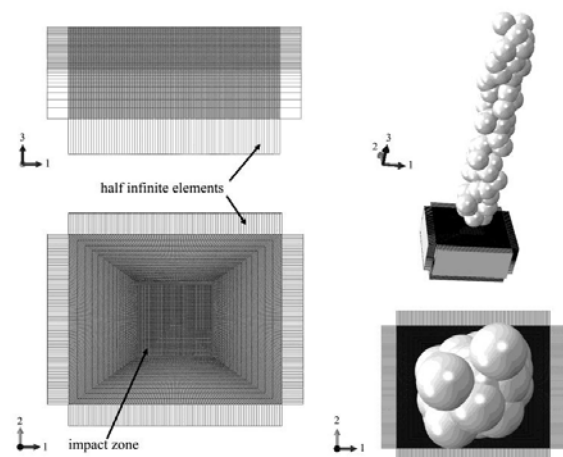


Fig.4. 3D shot peening model

In both models, shots were modelled as rigid solids with a density of 7800 kg/m^3 . Obviously, modelling the shots as elasto-plastic solids would increase the accuracy of our results [6, 7] but also the computational cost would highly increase, especially in 3D multi-impact simulations with full coverage [6]. However, a single-shot impact at a shot velocity of 45 m/s (close to the experimental one: 44 m/s) was simulated using three different values of the shot stiffness, an elastic-plastic shot model ($E = 210 \text{ GPa}$, $\sigma_y = 1500 \text{ MPa}$, $\sigma_u = 1850 \text{ MPa}$) in order to compare these results with the simulation considering rigid shots.

Table 7. Numerically obtained dimple diameter using different shot models

Shot model	Shot rate(m/s)	Dimple diameter (μm)
Elastic ($E = 165 \text{ GPa}$)	45	263.8
Elastic ($E = 240 \text{ GPa}$)	45	263.9
Elastic ($E = 480 \text{ GPa}$)	45	264
Rigid	45	264
Elastic-plastic	45	261.8

Table 7 gathers the obtained results. It can be seen that there are not significant differences in dimple diameter. Furthermore, since the main objective of this paper is to analyse the significant effect of the material model used to describe the target material behaviour in the numerical model rather than the accuracy level of the results, the use of rigid shot could be justified. In the axisymmetric model, the shot diameter was varied between 0.6 and 1 mm, while the velocity ranged between 30 and 100 m/s . In accordance with the experimental measurements, the shot diameter was set at 0.8 mm and the velocity at 40 m/s for the 3D model.

The coefficient of friction between the shots and the material was set at $\mu = 0.4$ [7]. A 90° impact

angle was used in order to maximize the impact energy transferred to the surface [29, 30]. The target material was modelled using the different models proposed in Section 2.2.2. In conventional shot peening treatment, total coverage must be achieved. This means that 98% of the treated surface has suffered at least one impact. The 3D model therefore has to reproduce a random number of impacts which ensures that total coverage is achieved. To assess the amount and the coordinates of the shots, first it is needed to obtain the dimple surface produced by these shots. This can be obtained following the subsequent steps. First is needed the experimental measurement of the size of the dimples, or the simulation of one shot in the axisymmetric model (assuming that the dimple is circular). Then, an algorithm has to be implemented in order to determine the number and the coordinates of the shots which ensure total coverage of the surface. A MATLAB routine was implemented for this purpose. The model inputs were the dimple diameter, shot velocity and target surface (1 mm^2 impact zone). Several assumptions were made: shots were not allowed to interact with each other and a constant velocity was assumed. Furthermore, the impact angle was set at 90° . In order to stabilize the material response, a separation of $2 \mu\text{s}$ was needed between each consecutive shot (this fact only influences the z coordinate). The x and y coordinates were distributed pseudo-randomly by means of the built-in random function of MATLAB.

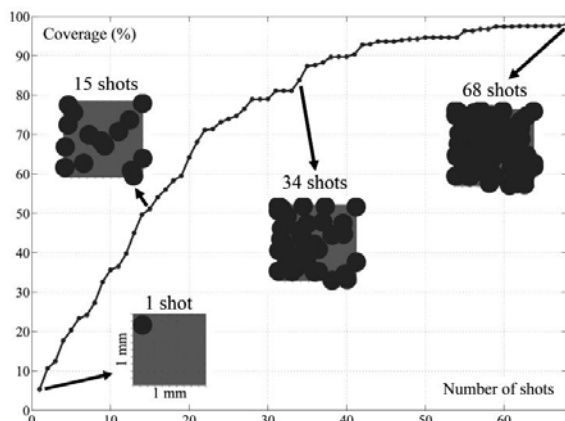


Fig.5. Example of the application of the MATLAB routine developed to assess shot coordinates. (Inputs: dimple diameter= $260 \mu\text{m}$; shot velocity= 40 m/s ; target surface= 1 mm^2)

Fig.5 graphically shows how the algorithm works. If the routine algorithm is run several times, a different number of required shots is obtained due to the random generation of the shot coordinates. However, a range can always be defined for the

amount of shots between a minimum (non-conservative solution) and a maximum (ultra-conservative solution). A good approach seems to be to consider an intermediate solution.

4 Results and discussion

4.1. Axisymmetric model: prediction of shot velocity

In the case of the axisymmetric model, only the effect of a single impact was assessed, since the desired result is the size of dimple generated after impact, instead of the residual stress field induced below the impacted surface.

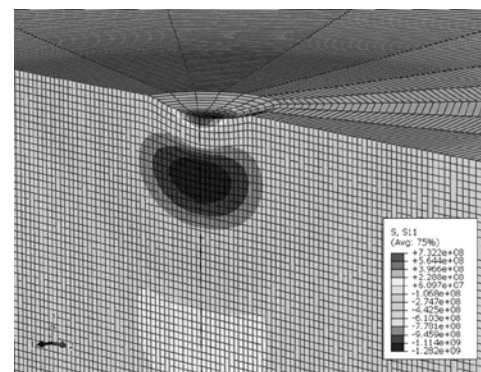


Fig.6. Field of residual stress created after a single impact

Thus, if the former stress profile is represented as in Fig.6, a tensile stress zone can be observed. This is in good agreement with the results of other researchers [30, 31], but it is not representative of the final state of the material after an actual shot peening treatment, involving total coverage. Nevertheless, Fig.6 can be used to appreciate the large volume of material affected by a single shot of 0.8 mm in diameter projected at 40 m/s onto the surface and the creation of a zone subjected to compressive stress. In this particular case, using the Johnson–Cook model, the size of this zone was around 250% the diameter of the dimple. However, the most important application of the proposed axisymmetric model was to obtain the diameter of the dimple generated after one single impact. This diameter can be easily obtained by measuring the distance between two opposite nodes located on the surface of the strip, with negative displacement being plotted on the y -axis. Fig.7 shows the profile of vertical displacements (U_3) generated by the impact of a single shot of 0.8 mm diameter projected at 40 m/s onto the material modelled with the Johnson–Cook model. Employing this numerical procedure, the measured dimple diameter was 242

μm , with an error of $\pm 12 \mu\text{m}$ due to the element size in this zone.

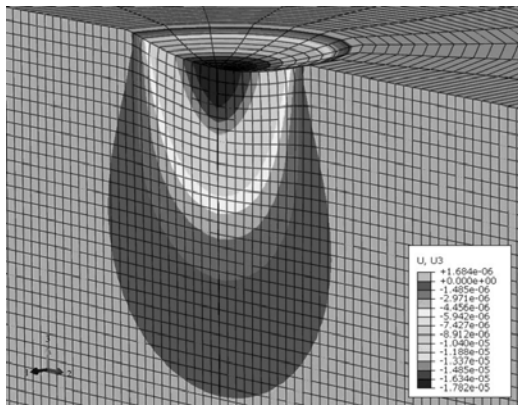


Fig.7. Vertical displacements induced by a single shot impact

Due to its low computational cost, the axisymmetric model can be used to assess the accuracy of different viscoplastic constitutive models which take into account the strain rate effect: the Cooper–Symonds and Johnson–Cook models and their modified proposals [14–17]. Furthermore, if the effect of an isolated impact is analysed, it would not be necessary to take into account the effect of the cyclic behaviour of the material. The accuracy of the models could be evaluated by comparing the numerical results with the experimental ones described in Section 3.1. Fig.8 summarizes the dimple diameters obtained numerically as a function of the applied shot velocities. As expected, an increase in velocity causes an increase in dimple diameter. The value of the dimple diameter obtained experimentally ($260 \pm 10 \mu\text{m}$) using a velocity of 44 m/s (Section 3.1) is also plotted in Fig. 8.

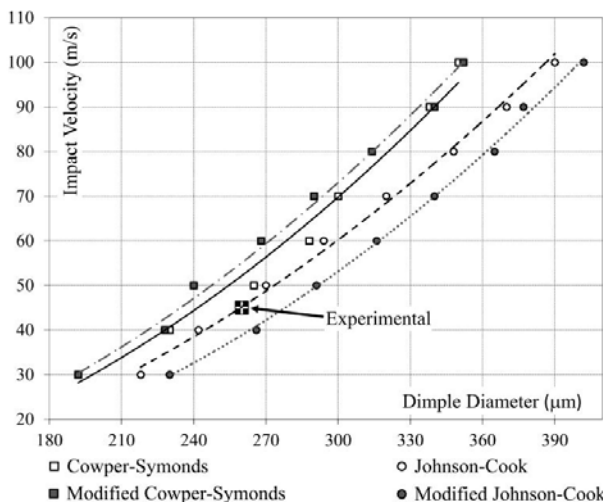


Fig.8. Dimple diameter vs Impact velocity for different viscoplastic constitutive models

Observation of this figure allows us to state that the most accurate result for measuring dimple diameter is obtained, in this case, using the Johnson–Cook model. Thus, the proposed axisymmetric model is an excellent tool to predict shot velocity as a function of dimple diameter.

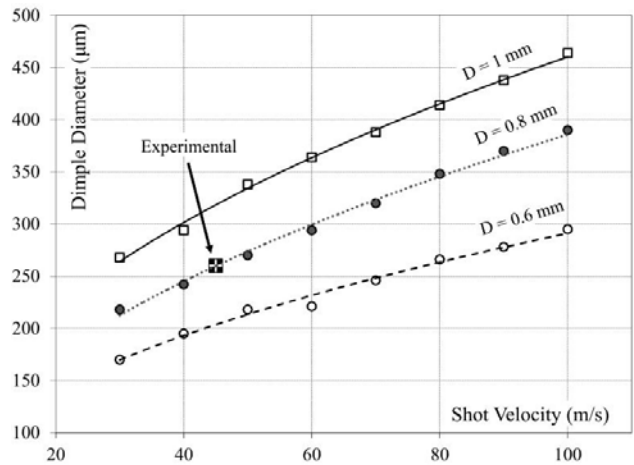


Fig.9. Dimple diameter vs shot velocity for the Johnson–Cook model

Fig.9 shows the plots of three different shot diameters: 0.6, 0.8 and 1 mm. Just by knowing the shot size and the dimple diameter, which are easily obtained experimentally, the shot velocity can be deduced by simply referring to the right shot size curve. Otherwise, the experimental measurement of the shot velocity involves a high degree of complexity despite the existence of several proposals.

4.2. 3DModel: effect of the constitutive material model

This model allows us to obtain the evolution of the residual stress in the depth direction (residual stress profile) as well as the surface roughness. It also enables us to define the validity of the different material models. Fig.10 shows the final appearance of the material under study after being impacted by 74 shots of 0.8 mm in diameter projected at 40 m/s onto a 1 mm² surface impact zone. As a result of the random sequence of multiple impacts, the target surface does not show a completely uniform distribution of residual stresses. Given that stresses measured by X-Ray diffraction are usually an average value of stresses in the area covered by X-Rays, multiple impact simulation results were compared with XRD measurements using a method suggested by Schwarzer. In this method, the mean residual stress in an area equal to the area affected by the X-rays is calculated at each depth. The

chosen area in the finite element model, shown in Fig.10, is a square area measuring $0.5 \times 0.5 \text{ mm}^2$ in the central zone of the impact area.

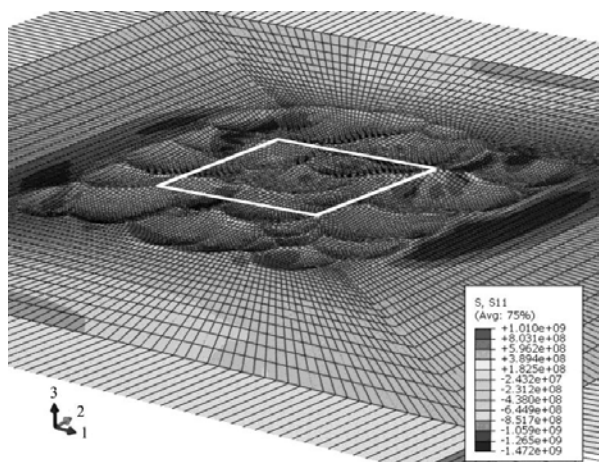


Fig.10. Appearance of the peened strip and area of residual stress measurement

Within this area, the value of the stress at a certain depth is calculated as the average of the stress components at the integration-Gauss points for all adjacent elements parallel to surface.

The characteristic profile of compressive residual stresses was then obtained using the aforementioned technique for each layer of elements.

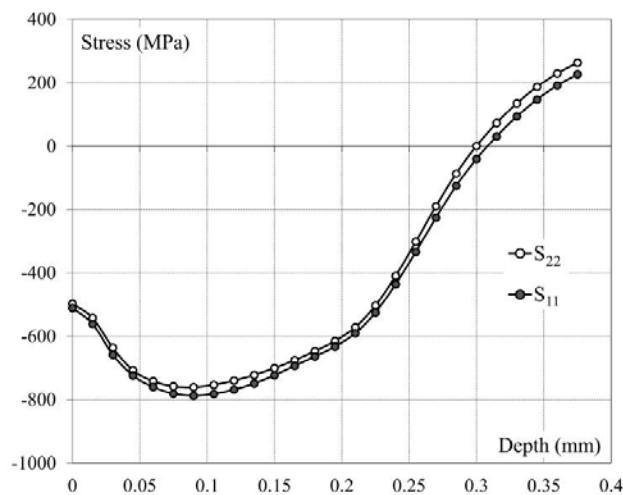


Fig.11. Residual stresses profiles obtained in two perpendicular directions (measurement zone: $1 \times 1 \text{ mm}^2$)

Fig.11 shows the residual stresses profiles obtained in two in-plane orthogonal directions (S_{11} , S_{22}). Both curves virtually overlap, indicating that, for the analysed area, the stresses are independent of the measuring direction and therefore the model is an accurate representation of an actual shot peening treatment. If the size of the measurement zone is reduced from $0.5 \times 0.5 \text{ mm}^2$ to $0.25 \times 0.25 \text{ mm}^2$ and the impact zone of $1 \times 1 \text{ mm}^2$ is kept constant, the results

are different. As can be observed in Fig.12, the values of S_{11} and S_{22} are very similar from a depth higher than 0.20 mm. However, considerable disagreement was observed within the more external layers. The aforementioned difference indicates that decreasing the measurement zone is not recommendable for the material under study and for this specific peening treatment. The rationale underlying this behaviour is that the outer layers of the material are more sensitive to the particular sequence of impacts and excessive reduction of the measurement zone leads to non-representative results.

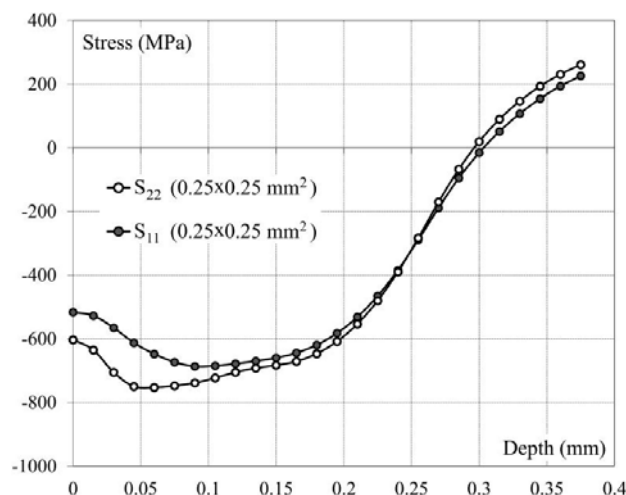


Fig.12. Residual stress profiles obtained in two perpendicular directions (measurement zone: $0.5 \times 0.5 \text{ mm}^2$)

Once the correct measure procedure to obtain the numerical stress had been established, the influence of the constitutive material model used in simulations was assessed by comparing the numerically predicted stress profiles for different models (Section 2.2) with the experimental (DRX) findings. Fig. 13 shows these results. The best prediction is obtained when the material's behaviour is simulated using the proposed constitutive model which takes into account both the strain rate and cyclic loading effects. As Fig. 13 shows and in line with the results reported by other authors [11], when the material is described using a model that only takes into account the strain rate effect (isotropic Johnson–Cook Model), the numerical prediction overestimates the residual stress profile induced by shot peening. On the other hand, if the material model only takes into account the cyclic loading effect (Chaboche Model), the numerical results underestimate experimental findings. However, if the model simultaneously takes into account the effects of the strain rate and cyclic loading (proposed model), considerable concordance

between numerical and experimental results is found. This model predicts a surface compressive stress of -511 MPa, which is in excellent agreement with the experimental result of -523 MPa. It should be noted that this is one of the most important results to obtain after shot peening treatment. Moreover, the maximum compressive stress obtained by means of the simulation, -787 MPa, is actually a good approximation of the measured value obtained from X-ray diffraction, -722 MPa. It is also worth noting that the depth at which this maximum stress is achieved is almost the same in both cases, 0.08 mm.

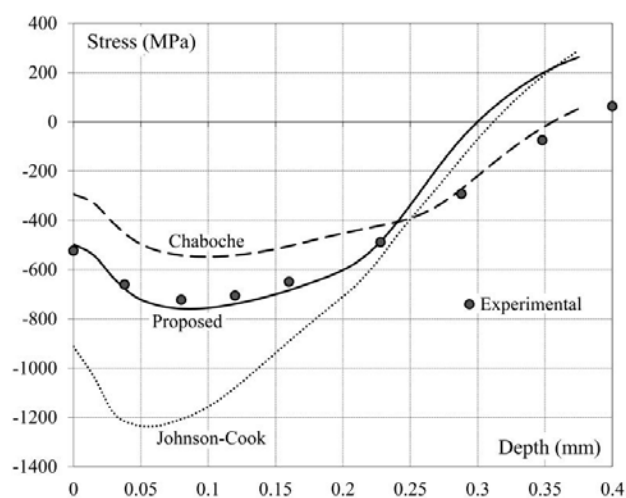


Fig.13. Numerical and experimental residual stress profiles

The only disagreement between the stress predicted by this model and experimental results can be observed in Fig. 13 for a depth greater than 0.25 mm. From this depth on, the proposed model provided residual stress values lower than those obtained experimentally, which, however, are closer to those proposed using the Chaboche model. The reason for this disagreement may lie in the fact that the proposed model overweights the strain rate effect versus cyclic hardening from a certain depth on. In addition, in this study we considered only one cyclic hardening law, the parameters of which correspond to a certain strain amplitude ($\Delta\varepsilon = \pm 0.09$). However, the cyclic hardening law could vary depending on the strain amplitude considered. Future work should focus on the analysis of the influence of different Chaboche parameters, depending on the in-use levels of plastic deformation.

Finally, the numerical surface roughness was assessed using the vertical displacements (U_3) of the surface nodes. The numerical value of the roughness parameter R_t can thus be approximated by the following expression:

$$R_t = \max(U_3) - \min(U_3) \quad (4)$$

Where $\max(U_3)$ and $\min(U_3)$ are, respectively, the highest peak and the deepest valley in the measurement zone (0.5×0.5 mm²) of the peened target surface. Fig. 14 shows the vertical displacement field after the shot peening treatment. As can be appreciated, the roughness results are strongly dependent on the measurement technique.

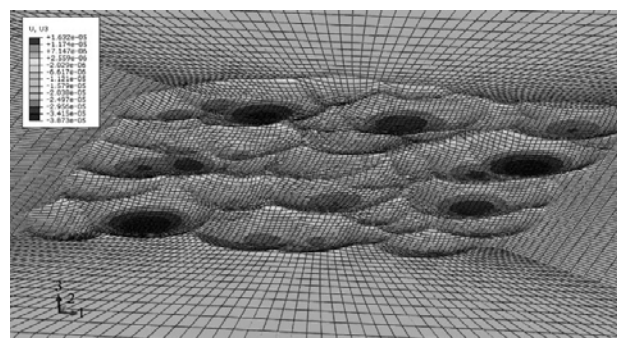


Fig.14 Vertical displacement of the surface nodes after the peening treatment

When all the nodes in the surface impact zone were considered, the average value of R_t was 44.1 μm . This result does not fit the experimental results obtained by means of both a roughness tester and a confocal microscope (Section 3.1). This difference may be explained by the different roughness measurement techniques used in each case. While the experimental measurement of roughness using the roughness tester only takes into account the values of peaks and valleys in a given measurement line of 0.45 mm in length (or in a very small area when using the confocal microscope), the numerical results are based on all values of the target area. A better comparison of experimental and numerical roughness measurements can be achieved if the same approach is used. It should be noted that if the vertical displacements (U_3) of 42 aligned surface nodes are obtained by means of the definition of different measurement straight lines of 0.5 mm in length, the results vary considerably, giving an average R_t value of 18.9 μm (average value of 6 measurement lines). This numerical roughness value shows a much better agreement with the experimental value ($\cong 16$ μm). In line with these observations, it may thus be concluded that roughness results also support the good predictions of the constitutive model proposed in this paper.

5 Conclusions

In this paper, an AISI 2205 duplex stainless steel was described by means of a non-linear kinematic

isotropic model which also takes into account the effect of the strain rate through its isotropic component.

By means of a 3D numerical simulation, it has been shown that the proposed model can reproduce the behaviour of the material subjected to an actual shot peening treatment, providing a very accurate prediction of both, residual stresses fields and surface roughness, generated by the shot peening process.

In addition, an axisymmetric numerical model has been proposed. Its low computational cost makes it a very useful tool for predicting the shot impact rate in a shot peening process (a parameter that is very difficult to obtain experimentally).

References:

- [1] SAE, *Manual on Shot Peening*, 2001.
- [2] J. Champaigne, Shot peening overview, *The Shot Peener*, 2001.
- [3] M. Klemenz, et al., Similarity rules for the shot peening process based on finite element simulations. *Proc. 9th Int. Conf. Shot Peening*, 2005, pp. 94–99.
- [4] M. Klemenz, et al. Application of the FEM for the prediction of the surface layer characteristics after shot peening. *Mater. Process. Technol.* 2009, pp. 4093–4102.
- [5] T. Hong, J.Y. Ooi, B. Shaw, A numerical simulation to relate the shot peening parameters to the induced residual stresses. *Eng. Fail. Anal.* 15, 2008 pp. 1097–1110.
- [6] T. Kim, H. Lee, H.C. Hyun, S. Jung. A numerical simulation to relate the shot peening parameters to the induced residual stresses. *Mater. Sci. Eng. A* 528, 2011, pp. 5945–5954.
- [7] T. Kim, H. Lee, H.C. Hyun, S. Jung, Effects of Rayleigh damping, friction and rate-dependency on 3D residual stress simulation of angled shot peening *Materials & Design.* 43, 2013, pp. 26–37.
- [8] M. Meo, R. Vignevic, Finite element analysis of residual stress induced by shot peening process *Adv. Eng. Softw.* 34, 2003, pp. 569–575.
- [9] G. Majzoobi, R. Azizi, A. Alavinia, *J. Mater. Process. Technol.* 2005, pp. 11229–11234.
- [10] S. Bagherifard, R. Ghelichi, M. Guagliano, *Surf. Coat. Technol.* 2010, pp. 4081–4090.
- [11] S.M.H. Gangaraj, M. Guagliano, G.H. Farrahi, A numerical model of severe shot peening (SSP) to predict the generation of a nanostructured surface layer of material *Surf. Coat. Technol.* 2014, pp. 39–45.
- [12] ASTM E8-04, Standard Test Methods for Tension Testing of Metallic Materials, 2004.
- [13] ASTM, *Standard Recommended Practice for Constant-Amplitude Low-Cycle Fatigue Testing*, 1980.
- [14] G. Cowper, P. Symonds, Strain hardening and strain-rate effects in the impact loading of cantilever beams, *Brown University Division of Applied Mathematics Report*, 1957.
- [15] G. Johnson, W. Cook, A Constitutive Model and Data for Metals Subjected to Large Strains, High Strain Rates and High Temperatures. *Proc. of 7th Int. S. On Bal*, 1983, pp. 541–547.
- [16] M. Alves, Material Constitutive Law for Large Strains and Strain Rates. *J. Eng. M.* 126 (2), 2000, pp. 215–218.
- [17] Kang, Modified Johnson–Cook Model for Vehicle body Crashworthiness Simulation, vol. 21, 1999.
- [18] J. Chaboche, *Int. J. Plast.* 24, 2008, pp. 1642–1693.
- [19] ABAQUS 6.12.1, 2014.
- [20] SAE J442, Test Strip, Holder and Gage for Shot Peening, *Society of Automotive Engineers*, 1995.
- [21] SAE J443, Procedures for Using Standard Shot Peening Test Strip, *Society of Automotive Engineers*, 1984.
- [22] MIL-S-13165C, *Shot Peening of Metal Parts*, 1989.
- [23] SAE J2441, *Shot Peening*, *Society of Automotive Engineers*, 2000.
- [24] P. Sanjurjo, *PHD Thesis*, Universidad de Oviedo, 2012.
- [25] W. Pfeiffer, *Proceedings of the 9th International Conference on Shot Peening*, 2005, pp. 414–419.
- [26] E. Real, *PHD Thesis*, Universidad de Oviedo, 2007.
- [27] K. Dai, et al., Finite element modeling of the surface roughness of 5052 Al alloy subjected to a surface severe plastic deformation process. *Acta Mater.* 52, 2004, pp. 5771–5782.
- [28] G. Mylonas, G. Labeas, Numerical modelling of shot peening process and corresponding products: Residual stress, surface roughness and cold work prediction. *Surf. Coat. Technol.* 205, 2011, pp. 4480–4494.
- [29] D. Kirk, Effect of varying shot impact angle, *The Shot Peener*, vol.19, 2005.
- [30] E. Rouhaud, A. Ouakka, C. Ould, J. Chaboche, M. Francois, *Proceedings of the 9th international conference on shot peening*, 2005, pp. 107–120.
- [31] M. Klemenz, V. Schulze, O. Vöhringer, D. Löhe, *Mater. Sci. Forum* 524–525, 2006, pp. 349–354.